

Accepted Manuscript

Synthesis of new Fe(II) and Ru(II) η^5 -monocyclopentadienyl compounds showing significant second order NLO properties

Andreia Valente, Sophie Royer, Milan Narendra, Tiago J.L. Silva, Paulo J.G. Mendes, M. Paula Robalo, Manuel Abreu, Jürgen Heck, M. Helena Garcia



PII: S0022-328X(13)00157-5

DOI: [10.1016/j.jorganchem.2013.02.028](https://doi.org/10.1016/j.jorganchem.2013.02.028)

Reference: JOM 17903

To appear in: *Journal of Organometallic Chemistry*

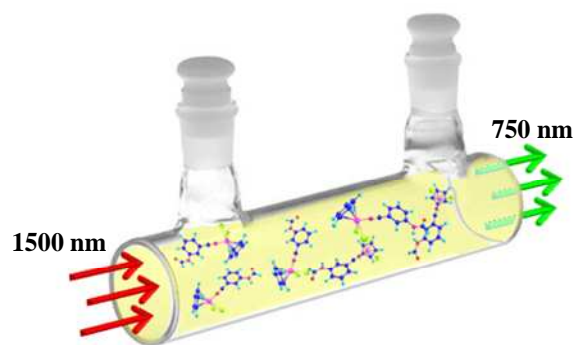
Received Date: 22 November 2012

Revised Date: 15 February 2013

Accepted Date: 21 February 2013

Please cite this article as: A. Valente, S. Royer, M. Narendra, T.J.L. Silva, P.J.G. Mendes, M.P. Robalo, M. Abreu, J. Heck, M.H. Garcia, Synthesis of new Fe(II) and Ru(II) η^5 -monocyclopentadienyl compounds showing significant second order NLO properties, *Journal of Organometallic Chemistry* (2013), doi: 10.1016/j.jorganchem.2013.02.028.

This is a PDF file of an unedited manuscript that has been accepted for publication. As a service to our customers we are providing this early version of the manuscript. The manuscript will undergo copyediting, typesetting, and review of the resulting proof before it is published in its final form. Please note that during the production process errors may be discovered which could affect the content, and all legal disclaimers that apply to the journal pertain.



ACCEPTED MANUSCRIPT

New organometallic Ru(II) and Fe(II) compounds revealed values in the $95\text{-}618 \times 10^3$ esu range by Hyper-Rayleigh Scattering (HRS) measurements at 1500 nm.

ACCEPTED MANUSCRIPT

Synthesis of new Fe(II) and Ru(II) η^5 -monocyclopentadienyl compounds showing significant second order NLO properties

Andreia Valente^a, Sophie Royer^b, Milan Narendra^a, Tiago J. L. Silva^{a,c}, Paulo J. G. Mendes^c, M. Paula Robalo^{b,d}, Manuel Abreu^e, Jürgen Heck^f, M. Helena Garcia^{a*}

^aCentro de Ciências Moleculares e Materiais, Faculdade de Ciências da Universidade de Lisboa, Campo Grande, 1749-016 Lisboa, Portugal

^bCentro de Química Estrutural, Complexo I, Instituto Superior Técnico, Av. Rovisco Pais, 1049-001 Lisboa, Portugal

^cCentro de Química de Évora, Universidade de Évora, Rua Romão Ramalho 59, 7002-554 Évora, Portugal

^dÁrea Departamental de Engenharia Química, Instituto Superior de Engenharia de Lisboa, Av. Conselheiro Emídio Navarro, 1, 1959-007 Lisboa, Portugal

^eLaboratório de Óptica, Lasers e Sistemas, Departamento de Física, Faculdade de Ciências da Universidade de Lisboa, Campo Grande, 1749-016 Lisboa, Portugal

^fInstitut für Anorganische und Angewandte Chemie, Universität Hamburg, Martin-Luther- King-Platz 6, D-20146 Hamburg

Abstract

A series of new ruthenium(II) complexes of the general formula $[\text{Ru}(\eta^5\text{-C}_5\text{H}_5)(\text{PP})(\text{L})][\text{PF}_6]$ (PP = DPPE or 2PPh_3 , L = 4-butoxybenzotrile or N-(3-cyanophenyl)formamide) and the binuclear iron(II) complex $[\text{Fe}(\eta^5\text{-C}_5\text{H}_5)(\text{PP})(\mu\text{-L})(\text{PP})(\eta^5\text{-C}_5\text{H}_5)\text{Fe}][\text{PF}_6]_2$ (L = (*E*)-2-(3-(4-nitrophenyl)allylidene)malononitrile, that has been also newly synthesized) have been prepared and studied to evaluate their potential in the second harmonic generation property. All the new compounds were fully characterized by NMR, IR and UV-Vis spectroscopies and their electrochemistry behaviour was studied by cyclic voltammetry. Quadratic hyperpolarizabilities (β) of three of the complexes have been determined by hyper-Rayleigh scattering (HRS) measurements at fundamental wavelength of 1500 nm and the calculated static β_0 values are found to fall in the range $65 - 212 \times 10^{-30}$ esu. Compound presenting $\beta_0 = 212 \times 10^{-30}$ esu has revealed to be 1.2 times more efficient than urea standard in the second harmonic generation (SHG) property, measured in the solid state by Kurtz powder technique, using a Nd:YAG laser (1064 nm).

Keywords

Cyclopentadienyl complexes; Quadratic hyperpolarizabilities; Hyper-Rayleigh scattering; Kurtz powder technique; Second-Order Nonlinear Optical

1. Introduction

There is current research interest in the development of second-order nonlinear optical (NLO) materials exhibiting large first hyperpolarizabilities β because of their applications

in laser frequency conversion, optical parameter oscillators and signal communication and the inherent employ in electrooptic devices.[1-9] The most intensively studied NLO chromophores are based in highly polarizable conjugated backbones presenting an electron donor and an acceptor group attached to both ends of the backbone in order to create an asymmetric “push-pull” system. Coordination of such systems to organometallic moieties bring additional possibilities to enhance high hyperpolarizabilities due to the occurrence of low energy ligand to metal or metal to ligand charge transfer. In this frame, the organometallic moiety forms an alternative type of donor or acceptor group for the traditional push-pull system. Additional advantages of complexes are related with the variation of coligands that can fine tune the energy of these charge transfer transitions besides the introduction of other variables related with size, nature and redox ability of the transition metal.

Our approach in the search of organometallic molecular materials with strong NLO properties has been based on “MCp” piano-stool structures where the chromophores are linked to the metal centre (Fe^{II} , Ru^{II} , Ni^{II} and Co^{III}) by functional groups such as nitrile ($\text{N}\equiv\text{C}$) or acetylide ($\text{C}\equiv\text{C}$) that allow interactions of the suitable metal d orbitals with the two π sets of orthogonal π and π^* orbitals of the functional group, leading consequently to an extension of the π -electron system between the metal and the terminal donor/acceptor substituting group of the ligand. Experimental values of the hyperpolarizabilities obtained by Hyper Rayleigh Scattering measurements were corroborated by our theoretical calculations, showing that “FeCp” and “RuCp” were the best partners for this kind of interaction, behaving more efficiently as electron donors than the traditional donor groups (such as alkyl substituted amine groups).[10] Within this prospective to search for a large NLO response in molecular materials, we continue to explore the field and we report here our recent results concerning four new compounds. As new approaches for structural

diversity and architectural flexibility we introduced a new structure designed to reinforce the π -backdonation effect through the pumping of electron density from two iron centres toward the same chromophore, and we also used the less classical chromophore N-(3-cyanophenyl)formamide.

The first hyperpolarizabilities (β) of the new compounds were measured by Hyper-Rayleigh Scattering with a laser emitting at 1500 nm. The NLO properties of the compound presenting the best static first hyperpolarizability (β_0) value was also studied in the solid state, by Kurtz powder technique, with a Nd:YAG laser emitting at 1064 nm.

2. Experimental

2.1. General procedures

All the experiments were carried out under dinitrogen atmosphere using standard Schlenk techniques. All the solvents used were dried using standard methods.[11] Starting materials $[M(\eta^5-C_5H_5)(LL)X]$ (LL = 2PPh₃ or DPPE, ethane-1,2-diylbis(diphenylphosphane), and X = Cl when M = Ru; LL = DPPE and X = I when M = Fe) were prepared following the methods described in the literature.[12,13] Compound N-(3-cyanophenyl)formamide (**L2**) was synthesised using an alternative method (see below) to the one published in [14]. Compound 4-butoxybenzotrile (**L1**) was purchased and used without further purification. FT-IR spectra were recorded in a Mattson Satellite FT-IR spectrophotometer with KBr pellets; only significant bands are cited in text. ¹H ¹³C and ³¹P NMR spectra were recorded on a Bruker Avance 400 spectrometer at probe temperature. The ¹H and ¹³C NMR chemical shifts are reported in parts per million (ppm) downfield from internal Me₄Si and the ³¹P NMR spectra are reported in ppm downfield from external standard, 85% H₃PO₄. Phase sensitive NOESY with gradients was

performed with a mixing time of 1.5 s at 45 °C. Elemental analyses were obtained at Laboratório de Análises, Instituto Superior Técnico, using a Fisons Instruments EA 1108 system. Data acquisition, integration and handling were performed using a PC with the software package EAGER-200 (Carlo Erba Instruments). Electronic spectra were recorded at room temperature on a Jasco V-560 spectrometer in the range of 200-900 nm.

2.2. Organic and organometallic synthesis

Synthesis of N-(3-cyanophenyl)formamide, L2

Compound N-(3-cyanophenyl)formamide was prepared by direct reaction of 3-cyanophenyl isocyanate with water in a yield of 95%.

IR (KBr, cm^{-1}): $\nu(\text{N-H stretch})$ 3367; $\nu(\text{C}\equiv\text{N, stretch})$ 2242; $\nu(\text{C-H, aldehyde stretch})$ 2800 and 2750; $\nu(\text{C=O, stretch})$ 1750. $^1\text{H NMR}$ [$(\text{CD}_3)_2\text{CO}$, Me_4Si , δ/ppm]: 8.57 [s, 1, COH]; 8.04 [s, 1, H_3]; 7.74 [d, 1, H_5]; 7.50 [t, 1, H_6]; 7.39 [d, 1, H_7]. $^{13}\text{C NMR}$ [$(\text{CD}_3)_2\text{CO}$, δ/ppm]: 153.1 (COH); 141.4 (C_4); 130.9 (C_6); 126.7 (C_7); 123.9 (C_5); 122.4 (C_3); 119.3 (C_1); 113.5 (C_2). UV-Vis in CH_2Cl_2 , $\lambda_{\text{max}}/\text{nm}$ ($\epsilon/\text{M}^{-1}\text{cm}^{-1}$): 273 (227504).

Synthesis of (E)-2(3-(4-nitrophenyl)allylidene)malononitrile, L3

The compound was synthesized by reaction of (E)-3-(4-nitrophenyl)prop-2-enal (0.02 mol) with malononitrile (0.02 mol) in methanol (40 mL) in the presence of piperidine (0.2 mL), during 2 h at room temperature. The product was filtrated, washed with water and dried under vacuum to give an orange solid product. Yield: 57%.

IR (KBr, cm^{-1}): $\nu(\text{NO}_2, \text{aromatic})$ 1516 + 1344; $\nu(\text{C}\equiv\text{N, stretch})$ 2225; $\nu(\text{C=C stretch conjugated})$ 1613. $^1\text{H NMR}$ [$(\text{CD}_3)_2\text{CO}$, Me_4Si , δ/ppm]: 8.32 [d, 2, H_9+H_{11}]; 8.17 [d, 1, H_4]; 8.08 [d, 2, H_8+H_{12}]; 7.73 [d, 1, H_6]; 7.53 [dd, 1, H_5]. $^{13}\text{C NMR}$ [$(\text{CD}_3)_2\text{CO}$, δ/ppm]: 161.1 (C_4); 149.9 (C_7); 148.1 (C_6); 141.4 (C_{10}); 130.7 (C_8+C_{12}); 127.0 (C_5); 125.0

(C₉+C₁₁); 114.3+112.3 (C₁+C₂); 85.7 (C₃). UV-Vis in CH₂Cl₂, λ_{max}/nm (ε/M⁻¹cm⁻¹): 268 (4732), 351 (17528). Anal. Calc. for C₁₂H₇N₃O₂: C, 64.00; H, 3.13; N, 18.66. Found: C, 64.32; H, 3.57; N, 17.08.

Preparation of ruthenium(II) complexes, [Ru(η⁵-C₅H₅)(PP)(NCR)][PF₆]

Complexes [Ru(η⁵-C₅H₅)(PP)(NCR)][PF₆] were prepared by halide abstraction from the parent neutral complexes [Ru(η⁵-C₅H₅)(PP)X] (0.5 mmol) with TlPF₆ (0.51 mmol) in dichloromethane, in the presence of a slight excess (0.51 mmol) of the ligands, **L1** and **L2**, at reflux for 6 h under inert atmosphere. After cooling to room temperature, filtering and removing the solvent, the complexes were washed with *n*-hexane (2 x 15 mL) and recrystallized from dichloromethane / *n*-hexane, giving crystalline yellow products.

*[Ru(η⁵-C₅H₅)(PPh₃)₂(L1)][PF₆], **1Ru***

Yellow; recrystallized from dichloromethane / *n*-hexane; 70 % yield; IR (KBr, cm⁻¹): ν(C≡N) absent, ν(PF₆⁻) 840 and 560. ¹H NMR [(CD₃)₂CO, Me₄Si, δ/ppm]: 7.46 [m, 6, PPh₃]; 7.36 [m, 14, PPh₃ + H₃ + H₇]; 7.25 [m, 12, PPh₃]; 7.08 [d, 2, H₄ + H₆]; 4.73 [s, 5, Cp]; 4.11 [t, 2, H₈]; 1.77 [m, 2, H₉]; 1.49 [m, 2, H₁₀]; 0.96 [t, 3, H₁₁]. ¹³C NMR [(CD₃)₂CO, δ/ppm]: 164.3 (C₅), 136.9-136.5 (C_q, PPh₃), 135.3 (C₃+C₇), 134.3 (C_{ortho}), 131.7 (C₁), 131.0 (C_{para}), 129.3 (C_{meta}), 116.4 (C₄ + C₆), 103.4 (C₂), 84.8 (Cp), 69.1 (C₈), 31.7 (C₉), 19.7 (C₁₀), 14.0 (C₁₁). ³¹P NMR [(CD₃)₂CO, δ/ppm]: 41.6 [PPh₃]; -144.2 [PF₆⁻]. UV-Vis in CH₂Cl₂, λ_{max}/nm (ε/M⁻¹cm⁻¹): 301 (26035), 374 (*sh*). UV-Vis in acetone, λ_{max}/nm (ε/M⁻¹cm⁻¹): 367 (*sh*). UV-Vis in DMSO, λ_{max}/nm (ε/M⁻¹cm⁻¹): 302 (19068), 370 (*sh*). Anal. Calc. for C₅₂H₄₈P₃F₆NORu: C, 61.78; H, 4.79; N, 1.39. Found: C, 61.4; H, 4.70; N, 1.30.

*[Ru(η⁵-C₅H₅)(DPPE)(L1)][PF₆], **2Ru***

Yellow; recrystallized from dichloromethane / *n*-hexane; 70 % yield; IR (KBr, cm^{-1}): $\nu(\text{C}\equiv\text{N})$ absent, $\nu(\text{PF}_6^-)$ 840 and 560. $^1\text{H-NMR}$ [$(\text{CD}_3)_2\text{CO}$, Me_4Si , δ/ppm]: 8.03 [m, 4, dppe]; 7.59 [m, 6, dppe]; 7.50 [m, 10, dppe]; 6.84 [d, 2, H_3+H_7]; 6.59 [d, 2, H_4+H_6]; 5.00 [s, 5, Cp]; 4.00 [t, 2, H_8]; 2.80 [m, 4, dppe]; 1.71 [m, 2, H_9]; 1.43 [m, 2, H_{10}]; 0.92 [t, 3, H_{11}]. $^{13}\text{C NMR}$ [$(\text{CD}_3)_2\text{CO}$, δ/ppm]: 164.0 (C_5), 138.0 (C_q , dppe), 134.8 (C_4+C_6), 134.2-129.8 (CH, dppe), 127.9 (C_1), 115.9 (C_3+C_7), 103.0 (C_2), 83.0 (Cp), 69.0 (C_8), 31.7 (C_9), 28.7-28.2 ($-\text{CH}_2-$, dppe), 19.7 (C_{10}), 14.0 (C_{11}). $^{31}\text{P-NMR}$ [$(\text{CD}_3)_2\text{CO}$, δ/ppm]: 79.35 [dppe]; -144.23 [PF_6^-]. UV-Vis in CH_2Cl_2 , $\lambda_{\text{max}}/\text{nm}$ ($\epsilon/\text{M}^{-1}\text{cm}^{-1}$): 287 (22941), 323 (*sh*). UV-Vis in acetone, $\lambda_{\text{max}}/\text{nm}$ ($\epsilon/\text{M}^{-1}\text{cm}^{-1}$): no bands are observed. UV-Vis in DMSO, $\lambda_{\text{max}}/\text{nm}$ ($\epsilon/\text{M}^{-1}\text{cm}^{-1}$): 292 (17103), 329 (*sh*). Anal. Calc. for $\text{C}_{43}\text{H}_{42}\text{P}_3\text{F}_6\text{NORu}$: C, 57.59; H, 4.72; N, 1.56. Found: C, 56.6; H, 4.70; N, 1.50.

*[Ru(η^5 -C₅H₅)(PPh₃)₂(L₂)]/[PF₆], **3Ru***

Yellow; recrystallized from dichloromethane / *n*-hexane; 50 % yield; IR (KBr, cm^{-1}): $\nu(\text{N-H, stretch})$ 3392; $\nu(\text{C}\equiv\text{N, stretch})$ 2233; $\nu(\text{C-H, aldehyde stretch})$ 2800 and 2750; $\nu(\text{C=O, stretch})$ 1750; $\nu(\text{PF}_6^-)$ 840 and 560. $^1\text{H NMR}$ [$(\text{CD}_3)_2\text{CO}$, Me_4Si , δ/ppm]: 8.0 [s, 1 H_3]; 7.7 [d, 1, H_5], 7.5-7.4 [m, 7, H_6+PPh_3]; 7.37 [m, 12, PPh_3]; 7.25 [m, 12, PPh_3]; 7.07 [d, 1, H_7]; 4.8 [s, 5, Cp]. $^{13}\text{C NMR}$ [$(\text{CD}_3)_2\text{CO}$, δ/ppm]: 154.4 (C_9); 141.4 (C_4); 136.8-136.3 (C_q , PPh_3), 134.2 (C_{ortho}), 131.1 (C_{para}), 131.0 (C_6), 129.4 (C_{meta}), 127.3 (C_7), 124.3 (C_5), 121.5 (C_3), 112.8 (C_2); 84.8 (Cp); CN is overlapped by phosphane signals. $^{31}\text{P-NMR}$ [$(\text{CD}_3)_2\text{CO}$, δ/ppm]: 41.40 [s, PPh_3]; -144,24 [sept, PF_6^-]. UV-Vis in CH_2Cl_2 , $\lambda_{\text{max}}/\text{nm}$ ($\epsilon/\text{M}^{-1}\text{cm}^{-1}$): 315 (16038). UV-Vis in acetone, $\lambda_{\text{max}}/\text{nm}$ ($\epsilon/\text{M}^{-1}\text{cm}^{-1}$): no bands are observed. UV-Vis in DMSO, $\lambda_{\text{max}}/\text{nm}$ ($\epsilon/\text{M}^{-1}\text{cm}^{-1}$): 317 (12910). Anal. Calc. for $\text{C}_{49}\text{H}_{41}\text{P}_3\text{F}_6\text{N}_2\text{ORu} \cdot \frac{1}{3}\text{CH}_3(\text{CH}_2)_4\text{CH}_3$: C, 60.61; H, 4.55; N, 2.77. Found: C, 60.1; H, 4.6; N, 2.8.

*Preparation of complex $[Fe_2(\eta^5-C_5H_5)_2(DPPE)_2(L3)][2PF_6]$, **1Fe***

$[Fe_2(\eta^5-C_5H_5)_2(DPPE)_2(L3)][2PF_6]$ was prepared by halide abstraction from the parent neutral complex $[Fe(\eta^5-C_5H_5)(DPPE)I]$ (0.5 mmol) with $TlPF_6$ (1.01 mmol) in dichloromethane, in the presence of a slight excess (0.51 mmol) of the ligand **L3**, at room temperature for 6 h under inert atmosphere. After cooling to room temperature, filtering and removing the solvent, the complex was washed with *n*-hexane (2 x 15 mL) and recrystallized from dichloromethane / *n*-hexane, giving a crystalline dark blue product in 50 % yield; IR (KBr, cm^{-1}): $\nu(C\equiv N, stretch)$ 2177, $\nu(PF_6^-)$ 840 and 560. (m); 557 (m); ^1H-NMR $[(CD_3)_2CO, Me_4Si, \delta/ppm]$: 8.31-7.29 [m, 44, $dpe_{1+2}+H_8+H_9+H_{11}+H_{12}$]; 7.01 [d, 1, H_6 ; $^3J_{56} = 16$ Hz]; 6.14 [d, 1, H_4 ; $^3J_{45} = 12$ Hz], 5.27 [dd, 1, H_5 ; $^3J_{56} = 16$ Hz; $^3J_{45} = 12$ Hz]; 4.67 [s, 5, Cp_2]; 4.57 [s, 5, Cp_1]; 3.09-2.60 [m, 8, dpe_{1+2}]. ^{13}C NMR $[(CD_3)_2CO, \delta/ppm]$: 157.2 (C_4), 149.9 (C), 145.9 (C_6), 141.4(C), 137.2 (C_q, dpe), 134.2-130.2 (-CH, dpe_{1+2}), 125.7 (C_5), 125.1 (-CH, dpe_1), 82.4 (Cp_1), 82.0 (Cp_2), 28.75+28.55(-CH₂-, dpe_{1+2}), CN is overlapped by phosphane signals. $^{31}P-NMR$ $[(CD_3)_2CO, \delta/ppm]$: 95.96 [s, dpe]; 94.49 [s, dpe]; -144.42 [sept, PF_6^-]. UV-Vis in CH_2Cl_2 , λ_{max}/nm ($\epsilon/M^{-1}cm^{-1}$): 359 (17566), 535 (*sh*), 628 (6364). UV-Vis in acetone, λ_{max}/nm ($\epsilon/M^{-1}cm^{-1}$): 356 (13590), 631 (5294). UV-Vis in DMSO, λ_{max}/nm ($\epsilon/M^{-1}cm^{-1}$): 360 (14113), 646 (6506). Anal. Calc. for $C_{74}H_{65}P_6F_{12}N_3O_2Fe_2.CH_2Cl_2$: C, 54.97; H, 4.12; N, 2.56. Found: C, 55.54; H, 4.15; N, 2.49.

2.3. Electrochemical experiments

The electrochemical experiments were performed on an EG&G Princeton Applied Research Model 273A potentiostat/galvanostat and monitored with a personal computer

loaded with Electrochemistry PowerSuite v2.51 software from Princeton Applied Research. Cyclic voltammograms were obtained using 10^{-3} M solutions of compounds in CH_2Cl_2 or CH_3CN , and 0.1 M of $[\text{NBu}_4][\text{PF}_6]$, with a three-electrode configuration. The working electrode was a platinum-disk (1.0 mm diameter) probed by a Luggin capillary connected to a silver-wire pseudo-reference electrode; a Pt wire auxiliary electrode was employed. The electrochemical experiments were performed under a N_2 atmosphere at room temperature. The redox potentials of the complexes were measured in the presence of ferrocene as the internal standard and the redox potential values are normally quoted relative to the SCE by using the ferrocenium/ferrocene redox couple ($E_{p/2} = 0.46$ or 0.40 V vs. SCE for CH_2Cl_2 or CH_3CN , respectively)[15].

The supporting electrolyte was purchased from Aldrich Chemical Co., recrystallized from ethanol, washed with diethyl ether and dried under vacuum at 110°C for 24 h. Reagent grade acetonitrile and dichloromethane were dried over P_2O_5 and CaH_2 , respectively, and distilled under nitrogen atmosphere before use.

2.4. HRS measurements

β measurements were carried out using the harmonic light scattering technique (also named Hyper-Rayleigh) in chloroform solutions. The 10^{-3} - 10^{-5} M solutions of the complexes were placed into a 4 cm long fluorimetric cell, after being carefully filtered through a 0.2 mm filter in order to eliminate the white light noise resulting from microburning of any the remaining dust particles by the incoming laser beam. The measurements were performed at a fundamental wavelength of 1500 nm as described in [16], using a Q-switched Nd:YAG laser operating in the 10 Hz repetition range. Instead of the third harmonic (355 nm) generated from an Nd:YAG laser with a wavelength of 1064 nm, the optical parametric oscillator (OPO)[17] in use was pumped with the second

harmonic (532 nm). The signal intensity at 824 nm and the fundamental at 532 nm were removed from the Idler using dichroic mirrors, a green-light filter (HR 532) and a silicon filter (HR 650–850; transparent > 1000 nm). An additional Glan-Taylor polariser ensured the vertical polarisation of the beam into the measurement cell. The scattered second harmonic signal is collected at 90° with respect to the direction of the incoming laser beam. The harmonic photons were detected by a photomultiplier, sampled by a boxcar and processed by a computer. A rotating a half-wave plate between two crossed polarizers varied the fundamental intensity. All measurements were carried out using Disperse Red 1 (DR1) as external standard. The reference hyperpolarisability β of DR1 in CH_2Cl_2 was calculated by comparison of the slopes of the standard in CH_2Cl_2 and CHCl_3 to obtain the ratio β_{solute} [18]. Using the value $\beta(\text{CHCl}_3) = 80 \times 10^{-30}$ esu[19] the hyperpolarisability of DR1 in CH_2Cl_2 is estimated to be 70×10^{-30} esu. The effect of the refractive indices of the solvents was corrected using simple Lorentz local field.[20] Assuming that the scattering contribution from the solvent is negligibly small, this external reference method is used to calculate the β values of chromophores according to eq. 1:

$$\beta = \sqrt{\frac{S_{\text{sample}}}{S_{\text{reference}}}} \quad (1)$$

where S is the slope of the appropriate “ I_{2w} vs. concentration” plot and β_{ref} is the orientational average of the first hyperpolarizability of the reference sample.

2.5. Kurtz powder SHG measurements

The efficiency of SHG was measured using the Kurtz powder method[21] using an alteration of our preceding experimental set-up published elsewhere[22], presented

in **Figure 1**. The powder sample S is located in a proper sample holder where it is exposed to a high-power pulsed laser beam. The sample is on the focus of the parabolic mirror R which collimates the rear lobule of the SHG light. The collimated beam is focused by the lens L on the silicon photo detector SPD. The sample holder has a line filter F of adequate wavelength for SHG in order to cut any leak due to the stray lighting (originated by the flash lamp), from the fundamental beam or residual fluorescence from the laser. Neutral density filters N, in the sample holder, allow control of the intensity of SHG light hitting the SPD. The SPD-signal is measured with a 2 GS⁻¹ digital oscilloscope DO which automatically integrates the signal. This integral is proportional to the SHG efficiency and a quantitative value is extracted by comparing it with its corresponding value from a reference material (urea) obtained under the same experimental conditions. The 1064 nm laser pulses are produced directly by the Nd:YAG laser at low power (110 mJ per pulse), this laser produces 10 ns pulses with a repetition rate of 4 Hz. Samples used in this experiment were not standardised both in the amount of test sample and grain size. For this reason signals between individual measurements were seen to vary in some cases by as much as $\pm 20\%$. The material to be measured was milled to a fine powder and compacted in a dedicated mount and then installed in the sample holder. For a proper comparison with the reference material, the measurements should be averaged over several laser exposure cycles. The signal amplitude from the SPD is measured by the oscilloscope, which is triggered by the signal itself. The silicon photo detector positioning and the neutral density filter were adjusted in order to obtain a good signal to noise ratio and to prevent saturation of the photodiode. The oscilloscope produces a time integral of the SPD waveform automatically, which is proportional to the SHG efficiency. The oscilloscope also performs the average over several laser shots

automatically. The reference sample SHG efficiency measurement is performed under the same experimental conditions as that of the test sample.

Figure 1. Experimental set-up for SHG measurements by Kurtz powder technique

3. Results and discussion

3.1. Synthesis of the M(II) complexes

Mononuclear complexes of the general formula $[\text{Ru}(\eta^5\text{-C}_5\text{H}_5)(\text{PP})(\text{L})][\text{PF}_6]$ with PP = DPPE or 2PPh₃, L = 4-butoxybenzotrile or N-(3-cyanophenyl)formamide, and the binuclear complex $[\text{Fe}(\eta^5\text{-C}_5\text{H}_5)(\text{PP})(\mu\text{-L})(\text{PP})(\eta^5\text{-C}_5\text{H}_5)\text{Fe}][\text{PF}_6]_2$ with L = (*E*)-2-(3-(4-nitrophenyl)allylidene)malononitrile) were prepared, as shown in

Scheme 1, by halide abstraction with TlPF₆ from the parent neutral complexes $[\text{M}(\eta^5\text{-C}_5\text{H}_5)(\text{PP})\text{X}]$ (M = Ru(II), X = Cl; M = Fe(II), X = I), in dichloromethane, in the presence of a slight excess of the corresponding ligand. The new bidentate ligand (*E*)-2-(3-(4-nitrophenyl)allylidene)malononitrile) (**L3**) was synthesised by reaction of (*E*)-3-(4-nitrophenyl)prop-2-enal with malononitrile in the presence of piperidine, at room temperature.

Scheme 1. Reaction scheme for the synthesis of the complexes $[\text{Ru}(\eta^5\text{-C}_5\text{H}_5)(\text{PP})(\text{L})][\text{PF}_6]$ and $[\text{Fe}(\eta^5\text{-C}_5\text{H}_5)(\text{PP})(\mu\text{-L})(\text{PP})(\eta^5\text{-C}_5\text{H}_5)\text{Fe}][\text{PF}_6]_2$ and the structures of the nitrile ligands numbered for NMR proposes

The reactions were carried out at reflux with exception of **1Fe** that was performed by stirring at room temperature for 6 h, under inert atmosphere. In the case of **L3** two approaches were used in order to obtain both the mononuclear and binuclear iron compounds. Nevertheless only the binuclear compound **1Fe** was obtained as pure

complex. The several attempts to synthesise the compound $[\text{Fe}(\eta^5\text{-C}_5\text{H}_5)(\text{DPPE})(\text{L3})]\text{PF}_6$ gave mixtures difficult to purify.

The new compounds were recrystallized by slow diffusion of *n*-hexane in acetone or dichloromethane solutions, giving crystalline yellow (**1Ru**, **2Ru** and **3Ru**) or dark blue products (**1Fe**). All the compounds are fairly stable to air and moisture in the solid state and were obtained in good yields (50-70%). The formulation of all the new compounds is supported by analytical data, FT-IR, ^1H , ^{13}C , ^{31}P NMR spectroscopic data and elemental analyses. The solid state FT-IR spectra (KBr pellets) of the complexes presented a large number of bands which identify the presence of the various coligands. Typical bands were used to confirm the presence of the cyclopentadienyl ligand (*ca.* 3100-3040 cm^{-1}) and the PF_6^- anion (840 and 560 cm^{-1}) in all the studied complexes. The disappearance of the $\nu_{\text{N}\equiv\text{C}}$ was observed upon coordination of **L1** to the ruthenium centre. However, in the case of the coordination of **L2** and **L3** ligands (the latter presenting the good NO_2 acceptor group) to the ruthenium and iron centre, respectively, negative shifts were observed (-9 cm^{-1} to **3Ru** and -48 cm^{-1} to **1Fe**). These negative shifts are indicative of an enhanced π -backdonation from the metal *d* orbitals to the π^* orbital of the $\text{N}\equiv\text{C}$ group leading to a decreased $\text{N}\equiv\text{C}$ bond order. This effect has been already observed in other ruthenium and iron related compounds.[23-25]

^1H NMR chemical shifts of the cyclopentadienyl ring are displayed in the characteristic range of monocationic ruthenium(II) and iron(II) complexes. Relatively to the ruthenium complexes a deshielding of the Cp protons between 0.47 and 0.68 ppm in relation the $[\text{RuCp}(\text{PPh}_3)_2\text{Cl}]$ precursor, can be observed. The same effect can be seen for the phosphane coligands.

The shielding effect on the nitrile ligand **L1** observed upon coordination to the ruthenium organometallic moiety became more evident for those protons adjacent to the $\text{N}\equiv\text{C}$ functional group, namely H_3 and H_7 protons (**Table 1**). Comparing the analogous complexes **1Ru** (presenting PPh_3 coligand) and **2Ru**, where the PPh_3 coligand was replaced by a better donor coligand, DPPE, this shielding effect was even extended to the H_4 and H_6 protons as well. Relatively to **3Ru**, where the previous nitrile chromophore **L1** was replaced by **L2**, while maintaining the PPh_3 coligand, one can observe a shielding of about -0.32 ppm on the H_7 proton, while the remaining aromatic protons do not suffer any change (**Table 1**). This shielding effect of π -backdonation was not observed in the other aromatic ring protons possibly due to the presence of the donor amine group in the *meta* position relative to the nitrile group.

The electron withdrawing effect of the NO_2 group in **1Fe** clearly causes an electronic delocalization throughout the coordinated ligand. Comparison of the chemical shifts of H_4 , H_5 and H_6 to those of the respective uncoordinated ligand **L3**, show that while these protons, closer to the $\text{C}\equiv\text{N}$ group, were severely shielded up to 2.27 ppm, the aromatic protons (H_8 , H_9 , H_{11} and H_{12}), nearby the NO_2 group, were not significantly affected (peak overlapping with DPPE coligand). The upfield shift observed for H_4 to H_6 protons confirms the expected shielding due to an electronic flow from the metal centre towards the NO_2 electron withdrawing group, due to a π -backdonation effect involving the coordinated nitrile group. This effect of π -backdonation was also confirmed by the $\text{N}\equiv\text{C}$ stretching frequencies on the infrared spectra of this compound, as discussed above.[23-25]

^{13}C NMR data for this family of compounds confirm the evidence found for proton spectra. The Cp ring chemical shifts are in the range usually observed for Ru(II) and Fe(II) cationic derivatives, a significant deshielding (up to ≈ 12 ppm) being observed on

the carbon of the N≡C functional group upon coordination. All the other carbons of the chromophore ligand were only slightly deshielded or remained almost unchanged for the studied compounds.

$^{31}\text{P}\{^1\text{H}\}$ NMR data of the ruthenium complexes showed a single sharp signal revealing equivalence of the coordinated phosphorous atoms, with the expected deshielding upon coordination, in accordance to the σ donor character of these ligands. For **1Fe**, two sharp signals corresponding to the DPPE coligand could be observed, consistent with the bimetallic character of this complex.

During NMR experiments a dependence on the temperature for complex **1Fe** has been observed (**Figure 2**). This effect has been attributed to an *E/Z* isomerisation and it is of particular interest since the hyperpolarizabilities of nonlinear optical chromophores depend on their geometrical *E/Z* isomerism.[26] In addition, when the chromophore possesses rotatable single bonds in the π -conjugated bridge, the influence of the rotation of these bonds on nonlinearity is significant and the rotational isomers (rotamers) exhibit different hyperpolarizabilities.[27] Analysing the coupling constants we can conclude that the predominant species at room temperature is the *E*-isomer ($J = 12\text{-}16\text{ Hz}$). Increasing the temperature one can observe the emerging of new ^1H NMR signals that can be attributed to the *Z*-isomer with coupling constants between 8-12 Hz (**Figure 2**). Moreover, a NOESY study allowed the observation of the spatial interactions between H_4 and H_6 protons (**Figure 3**), corroborating the hypothesis that the *E*-isomer is the predominant one.

Table 1. Selected ^1H NMR data for compounds $[\text{M}_n(\eta^5\text{-C}_5\text{H}_5)(\text{PP})(\text{L})][\text{PF}_6]_n$ and the free ligands

* Peak overlapping with DPPE

Figure 2. ^1H NMR spectrum of **1Fe** where the Z-isomer signals can be observed with increasing temperature

Figure 3. NOESY NMR spectrum for **1Fe**, showing spatial interaction between H_4 and H_6 protons

3.2. UV-Vis studies

The optical absorption spectra of the studied complexes $[\text{Ru}(\eta^5\text{-C}_5\text{H}_5)(\text{PP})(\text{L})][\text{PF}_6]$ and $[\text{Fe}(\eta^5\text{-C}_5\text{H}_5)(\text{PP})(\mu\text{-L})(\text{PP})(\eta^5\text{-C}_5\text{H}_5)\text{Fe}][\text{PF}_6]_2$ and all the ligands were recorded in $10^{-3} - 10^{-6}$ M dichloromethane, acetone and dimethyl sulfoxide solutions (**Table 2**) in order to identify MLCT and $\pi\text{-}\pi^*$ absorption bands expected for these complexes.

The electronic spectra of all the compounds showed intense absorption bands in the UV region, which can be assigned to electronic transitions occurring both in the organometallic fragment $\{\text{MCp}(\text{PP})\}^+$ ($\lambda \approx 235\text{-}260$ nm) and in the coordinated chromophore ($\lambda \approx 260 - 450$ nm) (**Table 2**). For compounds **3Ru** and **1Fe**, evidence was found for the existence of additional charge transfer (CT) bands. In fact, the iron complex presented one band compatible with a MLCT nature, this being confirmed by solvatochromism studies. As can be observed in the electronic spectra the compound **1Fe** (**Figure 4**) presents one MLCT broad band in DMSO. Changing the solvent polarity by replacing DMSO for dichloromethane, the enlargement of this band together with the appearance of one shoulder at higher energy is observed. Moreover, the bathochromic shift ($\bar{\nu} = 444$ cm^{-1}) in the main transition of this band is also compatible with its charge transfer nature. Nevertheless in the case of **3Ru** only one ILCT band can be observed, in

spite of the spectroscopic evidence ($^1\text{H NMR}$ and $\nu_{\text{NC}} = -9 \text{ cm}^{-1}$) that could suggest π -backdonation and therefore the possibility of existence of a MLCT band.

Table 2. Optical spectral data for complexes $[\text{M}_n(\eta^5\text{-C}_5\text{H}_5)(\text{PP})(\text{L})][\text{PF}_6]_n$, **1Ru**, **2Ru**, **3Ru**, **1Fe**, and the free ligands **L1**, **L2** and **L3**, in dichloromethane, acetone and dimethyl sulfoxide

Figure 4. Electronic spectra of complex **1Fe** and **L3** in CH_2Cl_2 and **1Fe** in DMSO showing the bathochromic shift for **1Fe**

3.3. Electrochemical studies

In order to obtain an insight on the electron richness of the organometallic fragment and on the coordinated ligands, the electrochemical behavior of Ru(II) and Fe(II) compounds and also the free chromophores **L1**, **L2** and **L3**, were studied by cyclic voltammetry in dichloromethane and acetonitrile, between the limits imposed by the solvents. Studies carried out at scan rates between 50 and 1000 mVs^{-1} showed the same results. **Table 3** summarizes the electrochemical data obtained for all the studied compounds at room temperature and at the scan rate of 200 mVs^{-1} .

The ligands **L1** and **L2** did not present any redox processes. The electrochemistry of **L3** in dichloromethane showed two irreversible reductive processes at -0.69 and -0.97 V respectively and three irreversible oxidative processes at $E_{\text{pa}} = +0.15$, -0.82 and -1.15 V. The oxidations were found not to be dependent of the reductive waves. The behaviour of

L3 in acetonitrile is similar showing the reductive processes in the range -0.67 and -1.28 V.

The bimetallic complex **1Fe**, in dichloromethane, displayed one quasi-reversible redox process at the potential expected for the redox Fe(II)/Fe(III) pair with $E_{1/2} = 0.94$ V, as was reported for related compounds[28,29]. Furthermore, two quasi reversible processes were found at $E_{1/2} \sim 0.08$ V and $E_{1/2} = -0.99$ V that can be related with ligand centred redox processes which became more reversible upon coordination to the iron(II) moieties. In acetonitrile, the complex **1Fe** showed decomposition during the electrochemical experiment, with the formation of the $[\text{Fe}(\eta^5\text{-C}_5\text{H}_5)(\text{DPPE})(\text{NCCH}_3)]^+$ species along time.

Complex **1Ru** present, in dichloromethane, one irreversible redox process occurring at the expected potential for Ru(II) oxidation ($E_{\text{pa}} = 1.32\text{V}$) and an irreversible reductive process at negative potentials $E_{\text{pc}} = -0.39$ V probably due to the coordinated ligand, which as free molecule did not present any redox process. The electrochemistry run in acetonitrile only showed one irreversible redox process ($E_{\text{pa}} = 1.06$ V) attributed to Ru(II)/Ru(III).

2Ru exhibited two redox processes at positive potentials and one irreversible reductive process at negative potentials in dichloromethane. The first positive redox process is quasi-reversible (at $E_{1/2} = 1.18$ V) when isolated, but the second one is irreversible with $E_{\text{pa}} = 1.54$ V. The reductive process occurring at negative potential ($E_{\text{pc}} = -0.26$ V) showed to be dependent from the second oxidative process. The electrochemical behaviour of **2Ru** in acetonitrile was characterized by a quasi-reversible redox process ($E_{1/2} = 1.08$ V) attributed to the redox pair Ru(II)/Ru(III).

The electrochemistry of **3Ru** also revealed one irreversible oxidation wave at $E_{pa} = 1.35$ V with a very small counterpart at $E_{pc} = 1.14$ V. The reduction of the coordinated ligand seemed to occur in a very irreversible way at $E_{pc} = -0.30$ V. This behaviour is very similar in acetonitrile.

The Ru^{II}/Ru^{III} potential is mainly affected by the phosphane coligand since the overall behaviour for the ruthenium compounds containing PPh₃ as coligand in both solvents was characterized by one oxidation process Ru(II)/Ru(III), with E_{pa} in the range 1.06 – 1.35 V with a very small cathodic counterpart, while for the dppe derivative, **2Ru**, the oxidation process Ru(II)/Ru(III) became quasi-reversible. Replacing PPh₃ by DPPE results in a decrease of ca. 0.10 V on the redox potential of the Ru(II)/Ru(III) couple (**1Ru** vs. **2Ru**), which agrees with the relative donating ability of the two phosphanes to the metal center. For the same phosphane, the Ru(II)/Ru(III) couple potential remains almost unchanged (**1Ru** vs. **3Ru**).

Table 3. Electrochemical data for the complexes $[M_n(\eta^5-C_5H_5)(PP)(L)][PF_6]_n$ and the free ligands in dichloromethane and acetonitrile

Figure 5. Cyclic voltammogram of complex **1Fe**, in dichloromethane solution, at 200 mV/s, showing the reversibility of the processes: - - - Fe(II)/Fe(III); Reduction of coordinated **L3**

3.4. Second order NLO properties

The second order nonlinear optical properties of the complexes **1Ru**, **3Ru** and **1Fe** were studied by hyper-Rayleigh scattering (HRS)[30] in diluted chloroform solutions (10^{-3} - 10^{-5} M). To avoid the effect of fluorescence due to two-photon absorption and to obtain as little resonance enhancement as possible[31], the stimulating laser light was shifted from the original wavelength of the used Nd:YAG laser of 1064 nm to a higher wavelength (1500 nm). Thus, a superposition of absorptions in the UV-Vis region and the SHG signal (750 nm) is reduced, which makes the calculated static hyperpolarisability (β_0)[31,32] more reliable.[16,33] Another important reason for using the higher wavelength incident beam, is an attempt to discriminate between a true SHG signal and a two photons absorption induced fluorescence (TPAF) enhanced signal.[20,34] At the 1500 nm incident beam HRS examinations were achieved using a tuneable optical parametric oscillator (OPO) based set-up.[16] The obtained molecular first hyperpolarizabilities β together with the corresponding calculated β_0 values are summarized in **Table 4**.

Table 4. Second-order NLO values for complexes **1Ru**, **3Ru** and **1Fe** at 1500 nm

$${}^a\beta_0 = \beta[1-(2\lambda_{\max}/1500)_2][1-(\lambda_{\max}/1500)_2]$$

Analysing the obtained values, compounds **1Ru** and **3Ru** present β_0 values quite close to the corresponding values of β since for both compounds the maximum of absorption is far from the second harmonic frequency (750 nm). Based on the spectroscopic evidences found for compound **1Fe** ($\Delta\nu_{\text{NC}} = -45 \text{ cm}^{-1}$; shielding on ${}^1\text{H}$ NMR up to ~ 2 ppm; solvatochromism at MLCT band centred at 628 nm) it would be expected a higher β value. However the calculation of β_0 gave a much lower value than expected. This can be explained by the strong broad optical transition in the visible range centred at 628 nm this affecting the β values by two-photon resonant enhancement. The well-known two-level

model (TLM) of Oudar and Chemla[31], which is very often used in the literature to derive static values, β_0 , is expected to become invalid close to resonance as it ignores any kind of line-broadening mechanisms. This model, in which it is assumed that the lowest energy CT transition yields the dominant contribution to β , diverges whenever the (laser or) second-harmonic wavelength approaches the transition wavelength. This can lead to a strong overestimation of the resonance effect and hence a significant underestimation of the static first hyperpolarizability.

Remarkably, compound **3Ru** presents a value of $\beta_0 = 212 \times 10^{-30}$ esu which places this complex in the range found for the best values of β_0 (200 - 400 $\times 10^{-30}$ esu) reported in the literature[12,35-38]. The absence of any MLCT absorption band led us to postulate that the quite significant value found for the first hyperpolarizability might be originated by variation of the dipolar moment between the ground state and the excited state related to the ILCT occurring at the coordinated ligand.

Motivated by the good β_0 value found for **3Ru**, we decide to measure the efficiency of second harmonic generation in the solid state using the Kurtz powder method[21], in spite of the inexistent information concerning the crystallographic space group due to difficulties to grow adequate single crystals. These measurements were performed at the Nd:YAG laser fundamental wavelength (1064 nm), due to the transparency of the sample at 532 nm, the second harmonic wavelength. It was found that compound **3Ru** was 1.2 times more efficient in doubling frequency than standard urea in the same experimental conditions. It is important to note that the results obtained by this technique depend not only on the molecular hyperpolarisability β , but also very strongly on the crystal packing structure, grain size, phase-matching properties, etc. Thus, this result can be explained on the assumption that compound crystallizes in a centric crystallographic group as happens with about 70% of the organic and organometallic compounds. At the light of these

results, it seems that compound **3Ru** can be considered with interesting NLO potential, and thus, further studies concerning several strategies envisaging acentric crystallization are in progress.

4. Conclusion

Four new ruthenium(II) and iron(II) piano stool structured complexes were synthesised in view to study their NLO properties. Spectroscopic data analysed on this scope suggested interesting potentiality as frequency doublers. Quadratic hyperpolarizabilities β were measured by Hyper Rayleigh Scattering at 1500 nm, showing values in the range 95-618 $\times 10^{-30}$ esu. The transparency observed in the visible region of compound **3Ru** gave a value of static hyperpolarizability of 212×10^{-30} esu, placing this compound in the best range of values reported in the literature. Studies in the solid state to study the ability of doubling a Nd:YAG laser beam of 1064 nm wavelength by Kurtz powder technique, showed that **3Ru** is 1.2 times more efficient than urea standard. Although a stronger effect would be expected considering the significant value of the found static hyperpolarizability, this result can be explained on the basis of a probable centric crystallization. Hence, further studies concerning several strategies to guarantee acentric crystallization for **3Ru** are currently in progress.

Acknowledgments

The authors thank financial support from the Portuguese Foundation for Science and Technology for the projects PTDC-QUI-66148-2006, PEst-OE/QUI/UI0536/2011 and

SFRH/BPD/80459/2011 (Andreia Valente's postdoctoral scholarship). Technical assistance involving Kurtz powder technique is thanked to Fernando Monteiro.

References

- [1] H. S. Nalwa, *Appl. Organomet. Chem.* 5 (1991) 349.
- [2] N. J. Long, *Angew. Chem. Int. Ed. Engl.* 34 (1995) 21.
- [3] S. R. Marder, in: D. W. Bruce, D. O'Hare (Eds.), *Inorganic Materials*, second ed., Wiley, Chichester, 1996, pp.121.
- [4] L. R. Whittal, A. M. McDonagh, M. G. Humphrey, M. Samoc, *Adv. Organomet. Chem.* 42 (1998) 291.
- [5] E. Goovaerts, W. E. Wenseleers, M. H. Garcia, G. H. Cross, in: H. S. Nalwa (Ed.), *Handbook of Advanced Electronic and Photonic Materials*, vol. 9, 2001, pp. 127 (Chapter 3).
- [6] S. Di Bella, *Chem. Soc. Rev.* 30 (2001) 355.
- [7] C.E. Powell, M.G. Humphrey, *Coord. Chem. Rev.* 248 (2004) 725.
- [8] E. Cariati, M. Pizzotti, D. Roberto, F. Tessore, R. Ugo, *Coord. Chem. Rev.* 250 (2006) 1210.
- [9] J.P. Morrall, G.T. Dalton, M.G. Humphrey, M. Samoc, *Adv. Organomet. Chem.* 55(2007) 61.
- [10] W. Wenseleers, A. W. Gerbrandij, E. Goovaerts, M. H. Garcia, M. P. Robalo, P. J. Mendes, J. C. Rodrigues, A. R. Dias, *J. Mater. Chem.* 8 (1998) 925.

- [11] D. D. Perrin, W. L. F. Amarego, D. R. Perrin, Purification of Laboratory Chemicals, 2nd ed., Pergamon, New York, 1980.
- [12] M. H. Garcia, M. P. Robalo, A. R. Dias, M. F. M. Piedade, A. Galvão, M. T. Duarte, W. Wensellers, E. Goovaerts, J. Organomet. Chem. 619 (2001) 252.
- [13] G. S. Ashby, M. I. Bruce, I. B. Tomkins, R. C. Walli, Aust. J. Chem. 32 (1979) 1003.
- [14] M. Hosseini-Sarvari, H. Sharghi, J. Org. Chem. 71 (2006) 6652.
- [15] N.G. Conelly, W.E. Geiger, Chem. Rev. 96 (1996) 877.
- [16] S. Stadler, R. Dietrich, G. Bourhill, C. Bräuchle, A. Pawlik, W. Grahn, Chem. Phys. Lett. 247 (1995) 271.
- [17] Paralite Optical Parametrical Oscillator, LAS GmbH.
- [18] T. Kodaira, A. Watanabe, O. Ito, M. Matsuda, K. Clays, A. Persoons, J. Chem. Soc., Faraday Trans. 93 (1997) 3039.
- [19] Z. Wu, R. Ortiz, A. Fort, M. Barzoukas, S. R. Marder, J. Organomet. Chem. 528 (1997) 217.
- [20] C. Lambert, G. Nöll, E. Schmäzlin, K. Meerholz, C. Bräuchle, Chem. Eur. J. 4 (1998) 2129.
- [21] S. K. Kurtz, T. T. Perry, J. Appl. Phys. 39 (1968) 3798.
- [22] M. H. Garcia, J. C. Rodrigues, A. R. Dias, M. F. M. Piedade, M. T. Duarte, M. P. Robalo, N. Lopes, J. Organomet. Chem. 632 (2001) 133.

- [23] A. R. Dias, M. H. Garcia, J. C. Rodrigues, M. L. H. Green, S. M. Kuebler, J. Organomet. Chem. 475 (1994) 241.
- [24] W. Wenseleers, A. W. Gerbrandij, E. Goovaerts, M. H. Garcia, M. Paula Robalo, Paulo J. Mendes, João C. Rodrigues, A. R. Dias, J. Mater. Chem. 8 (1998) 925.
- [25] A. R. Dias, M. H. Garcia, M. P. Robalo, M. L. H. Green, K. K. Lai, A. J. Pulham, S. M. Klueber, G. Balavoine, J. Organomet. Chem. 453 (1993) 241.
- [26] J. O. Morley, M. G. Hutchings, J. Zyss, I. Ledoux, J. Chem. Soc., Perkin Trans. 2 (1997) 1139.
- [27] T. Kinnibrugh, S. Bhattacharjee, P. Sullivan, C. Isborn, B. H. Robinson, B. E. Eichinger, J. Phys. Chem. B 110 (2006) 13512.
- [28] M. H. Garcia, P. J. Mendes, M. P. Robalo, A. Romão Dias, J. Campo, W. Wenseleers, E. Goovaerts, J. Organomet. Chem. 692 (2007) 3027.
- [29] M. H. Garcia, P. Florindo, M. F. M. Piedade, M. T. Duarte, M. P. Robalo, J. Heck, C. Wittenburg, J. Holtmann, E. Licandro, J. Organomet. Chem. 693 (2008) 2987.
- [30] K. Clays, A. Persoons, Rev. Sci. Instrum. 63 (1992) 3285.
- [31] J. L. Oudar, D. S. Chemla, J. Chem. Phys. 66 (1977) 2664.
- [32] E. Hendrickx, K. Clays, C. Dehu, J. L. Brédas, J. Am. Chem. Soc. 117 (1995) 3547.
- [33] J. J. Wolff, R. Wortmann, Adv. Phys. Org. Chem. 32 (1999) 121.
- [34] (a) K. Clays, E. Hendrickx, T. Verbiest, A. Persoons, Adv. Mater. 10 (1998) 643; (b) J. J. Wolff, R. Wortmann, J. Prakt. Chem. 340 (1998) 99; S. Stadler, R. Dietrich, G. Bourhill, C. Bräuchle, J. Phys. Chem. 100 (1996) 6927.

- [35] L. Labat, J.-F. Lamère, I. Sasaki, P. G. Lacroix, L. Vendier, I. Asselberghs, J. Pérez-Moreno, K. Clays, *Eur. J. Inorg. Chem.* (2006) 3105.
- [36] I. S. Lee, D. S. Choi, D. M. Shin, Y. K. Chung, C. H. Choi, *Organometallics* 23 (2004) 1875.
- [37] H. Le Bozec, T. Renouard, M. Bourgault, C. Dhenaut, S. Brasselet, I. Ledoux, J. Zyss, *Synthetic Metals* 124 (2001) 185.
- [38] I. R. Whittall, M. P. Cifuentes, M. G. Humphrey, B. Luther-Davies, M. Samoc, S. Houbrechts, A. Persoons, G. A. Heat, D. C. R. Hockless, *J. Organomet. Chem.* 549 (1997) 127.

‘Synthesis of new Fe(II) and Ru(II) η^5 -monocyclopentadienyl compounds showing significant second order NLO properties’

Manuscript reference: JOM 17903

Editorial reference: JOM_JORGANCHEM-D-12-00701

Highlights

- Four new ruthenium(II) and iron(II) piano stool structured complexes
- Spectroscopic data suggest interesting potentiality as frequency doublers
- Static β_0 values for the new complexes fall in the range 65 - 212×10^{-30} esu
- One compound is 1.2 times better than urea for 2nd harmonic generation (SHG)

- Four new ruthenium(II) and iron(II) piano stool structured complexes were fully characterized.
- Spectroscopic data analysed on the scope of NLO properties suggest interesting potentiality as frequency doublers.
- Quadratic hyperpolarizabilities β measured by Hyper Rayleigh Scattering at 1500 nm, showed values in the range $95\text{-}618 \times 10^{-30}$ esu.
- Static hyperpolarizability (β_0) of 212×10^{-30} esu places one of the compounds among the best values reported in the literature.
- One of the compounds is 1.2 times more efficient than urea standard in the second harmonic generation (SHG) property.

	H₃	H₄	H₅	H₆	H₇	H₈	H₉	H₁₀	H₁₁	H₁₂
L1	7.66	7.06	–	7.06	7.66	4.06	1.75	1.48	0.95	–
1Ru	7.36*	7.08	–	7.08	7.36*	4.11	1.77	1.49	0.96	–
2Ru	6.84	6.60	–	6.60	6.84	4.00	1.71	1.42	0.93	–
L2	8.04	–	7.74	7.50	7.39	–	–	–	–	–
3Ru	8.00	–	7.69	7.46*	7.07	–	–	–	–	–
L3	–	8.17	7.53	7.73	–	8.08	8.32	–	8.32	8.08
1Fe	–	6.14	5.27	7.01	–	*	*	–	*	*

Compound	λ_{\max} (nm) (ϵ , $M^{-1}cm^{-1}$)		
	CH ₂ Cl ₂	Acetone	DMSO
1Ru	301 (26035)	–	302 (19068)
	374 (sh)	367 (sh)	370 (sh)
2Ru	287 (22941)	–	292 (17103)
	323 (sh)	–	329 (sh)
3Ru	315 (16038)	–	317 (12910)
1Fe	359 (17566)	356 (13590)	360 (14113)
	535 (sh)	–	–
	628 (6364)	631 (5294)	646 (6506)

	E_{pa} (V)	E_{pc} (V)	$E_{1/2}$ (V)	$E_{pa} - E_{pc}$ (mV)	i_{pc}/i_{pa}
--	-----------------	-----------------	------------------	---------------------------	-----------------

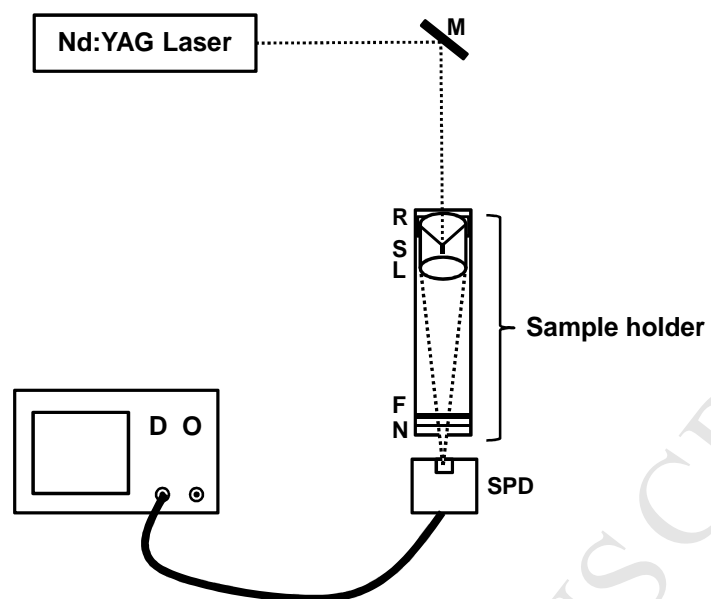
Dichloromethane

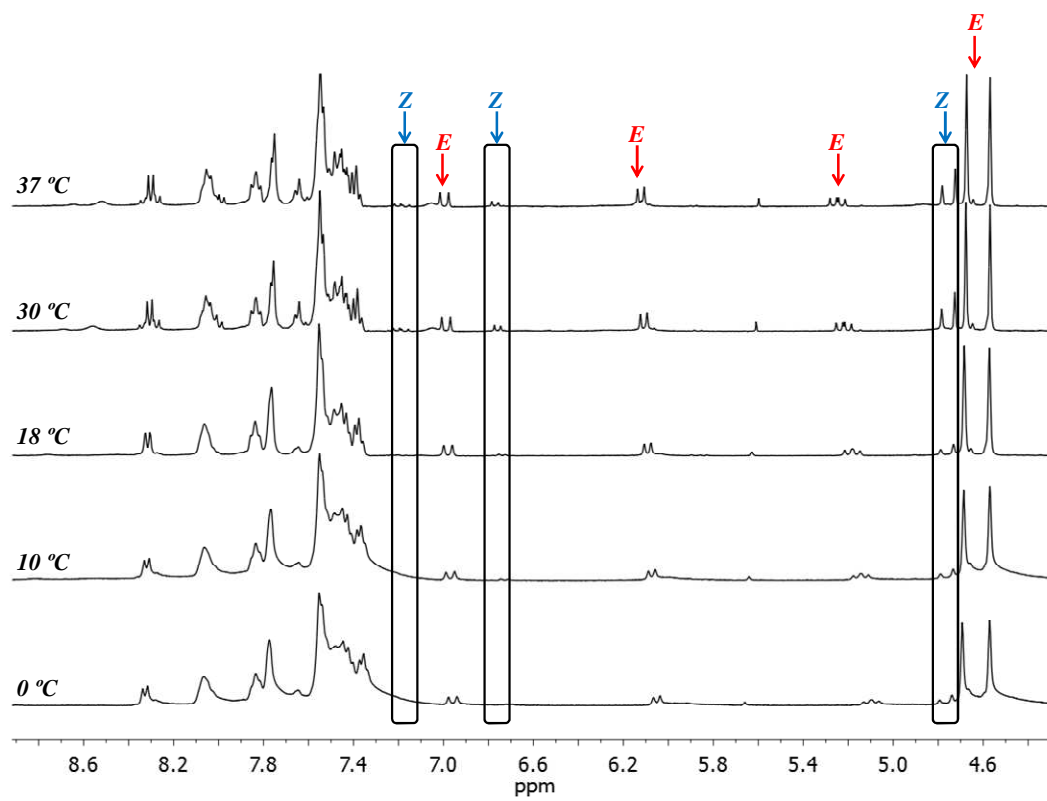
1Ru	1.32	1.08 -0.32			
2Ru	1.54 1.22	1.13 -0.26	1.18	90	0.9
3Ru	1.35	1.14 -0.30			
1Fe	0.97 0.13 -1.04	0.88 0.03 -0.45 -0.93	0.94 0.08 -0.99	90 100 110	0.95 1.0 1.0
L3	0.15 -0.82 -1.15	-0.69 -0.97			

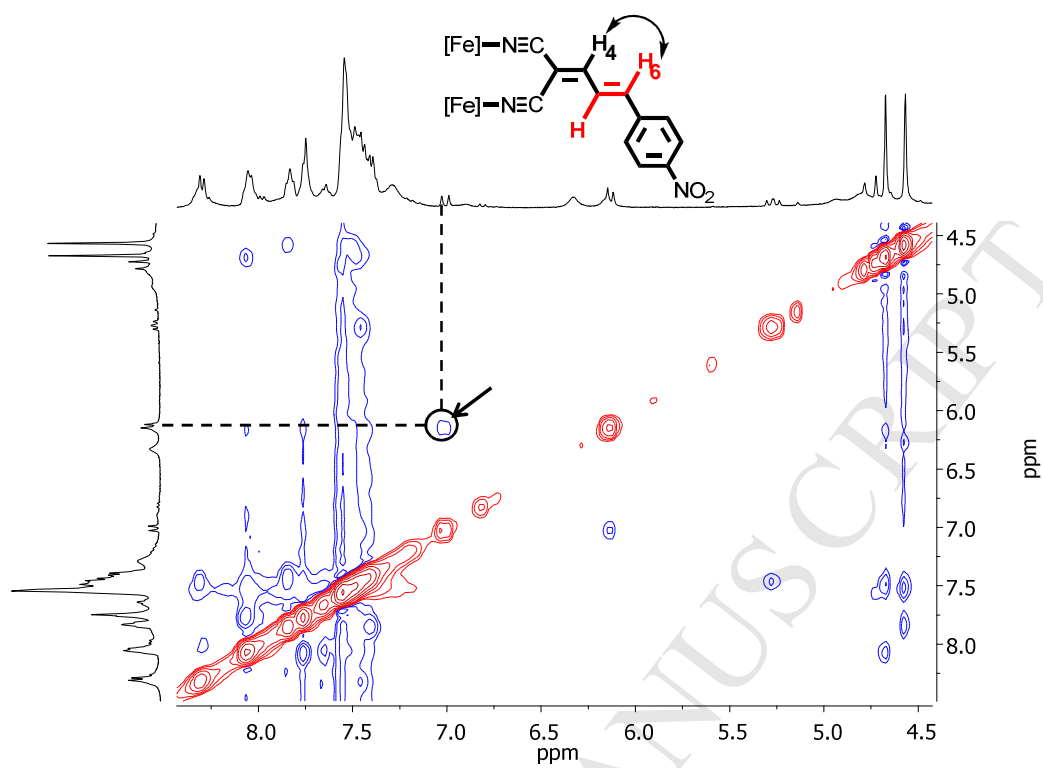
Acetonitrile

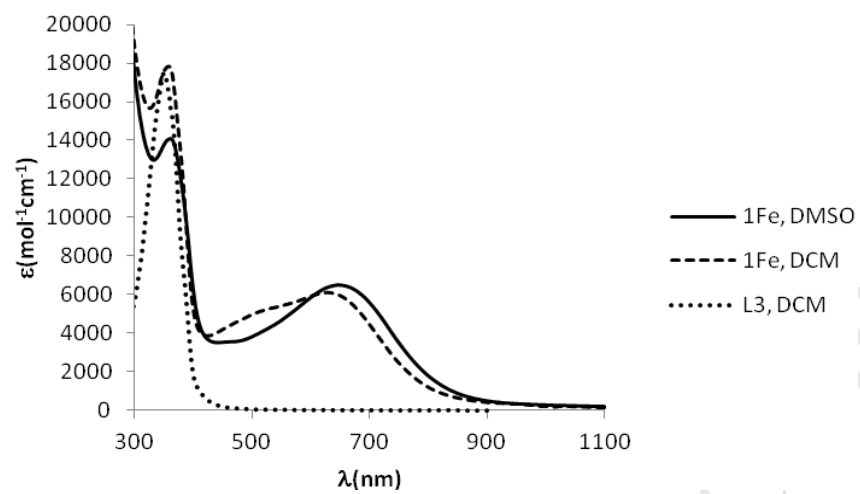
1Ru	1.06	0.93			
2Ru	1.18	1.10	1.14	80	1.0
3Ru	1.08	0.96			
L3	-0.81 -1.06	-0.67 -0.92 -1.28			

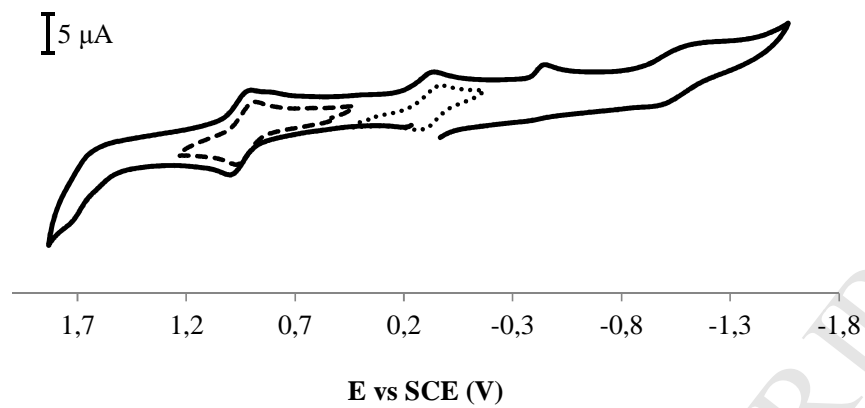
Compound	β ($\times 10^{-30}$ esu)	β_0^a ($\times 10^{-30}$ esu)	Max. Abs. (nm)
1Ru	95	65	374
3Ru	264	212	315
1Fe	618	116	628



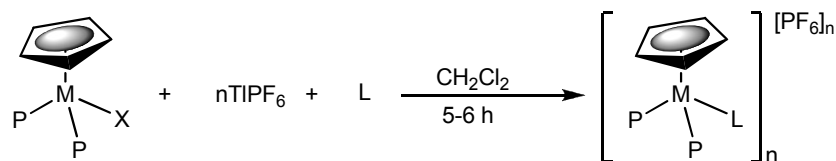




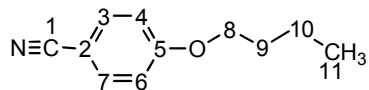
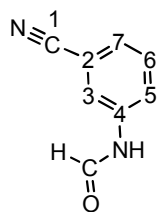
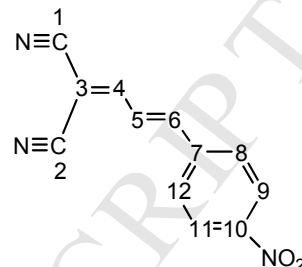




ACCEPTED MANUSCRIPT



L:

4-butoxybenzonitrile
(L1)N-(3-cyanophenyl)formamide
(L2)(E)-2-(3-(4-nitrophenyl)allylidene)-
malononitrile
(L3)

1Ru: n = 1; M = Ru; X = Cl; PP = 2PPh₃; L1
2Ru: n = 1; M = Ru; X = Cl; PP = DPPE; L1
3Ru: n = 1; M = Ru; X = Cl; PP = 2PPh₃; L2
1Fe: n = 2; M = Fe; X = I; PP = DPPE; μ-L3